

Cerebral blood flow and cerebrovascular reactivity correlate with severity of motor symptoms in Parkinson's disease

Laura Pelizzari¹, Maria Marcella Laganà, Federica Rossetto, Niels Bergsland, Mirco Galli, Giuseppe Baselli, Mario Clerici, Raffaello Nemni and Francesca Baglio²

Ther Adv Neurol Disord

2019, Vol. 12: 1–10

DOI: 10.1177/
1756286419838354

© The Author(s), 2019.
Article reuse guidelines:
sagepub.com/journals-
permissions

Abstract

Background: Parkinson's disease (PD) is a progressive neurodegenerative disorder that is mainly characterized by movement dysfunction. Neurovascular unit (NVU) disruption has been proposed to be involved in the disease, but its role in PD neurodegenerative mechanisms is still unclear. The aim of this study was to investigate cerebral blood flow (CBF) and cerebrovascular reactivity (CVR) within the regions belonging to the motor network, in patients with mild to moderate stages of PD.

Methods: Twenty-eight PD patients (66.6 ± 8.6 years, 22 males, median [interquartile range, IQR] Hoehn & Yahr = 1.5 [1–1.9]) and 32 age- and sex-matched healthy controls (HCs) were scanned with arterial spin labeling (ASL) magnetic resonance imaging (MRI) for CBF assessment. ASL MRI was also acquired in hypercapnic conditions to induce vasodilation and subsequently allow for CVR measurement in a subgroup of 13 PD patients and 13 HCs. Median CBF and CVR were extracted from cortical and subcortical regions belonging to the motor network and compared between PD patients and HCs. In addition, the correlation between these parameters and the severity of PD motor symptoms [quantified with Unified Parkinson's Disease Rating Scale part III (UPDRS III)] was assessed. The false discovery rate (FDR) method was used to correct for multiple comparisons.

Results: No significant differences in terms of CBF and CVR were found between PD patients and HCs. Positive significant correlations were observed between CBF and UPDRS III within the precentral gyrus, postcentral gyrus, supplementary motor area, striatum, pallidum, thalamus, red nucleus, and substantia nigra (pFDR < 0.05). Conversely, significant negative correlation between CVR and UPDRS III was found in the corpus striatum (pFDR < 0.05).

Conclusion: CBF and CVR assessment provides information about NVU integrity in an indirect and noninvasive way. Our findings support the hypothesis of NVU involvement at the mild to moderate stages of PD, suggesting that CBF and CVR within the motor network might be used as either diagnostic or prognostic markers for PD.

Keywords: arterial spin labeling, cerebral blood flow, cerebrovascular reactivity, Parkinson's disease

Received: 8 November 2018; revised manuscript accepted: 2 February 2019.

Introduction

Parkinson's disease (PD) is the most common progressive neurodegenerative disorder after Alzheimer's disease, affecting primarily the elderly (about 6.3 million people around the world). It is

characterized by early marked death of dopaminergic neurons in the substantia nigra pars compacta, which induces dopamine dysregulation in the corpus striatum, and eventually leads to movement dysfunction.¹ The core motor symptoms of

Correspondence to:

Francesca Baglio
IRCCS, Fondazione Don
Carlo Gnocchi, CADiTeR,
Via Alfonso Capecelatro
66, Milan, Italy
fbaglio@dongnocchi.it

Laura Pelizzari
IRCCS, Fondazione Don
Carlo Gnocchi, Milan, Italy

Maria Marcella Laganà
Federica Rossetto
Mirco Galli
IRCCS, Fondazione Don
Carlo Gnocchi, Milan, Italy

Niels Bergsland
IRCCS, Fondazione Don
Carlo Gnocchi, Milan, Italy
Buffalo Neuroimaging
Analysis Center,
Department of Neurology,
Jacobs School of Medicine
and Biomedical Sciences,
University at Buffalo, State
University of New York,
Buffalo, NY, USA

Giuseppe Baselli
Department of
Electronics, Information
and Bioengineering,
Politecnico di Milano,
Milan, Italy

Mario Clerici
Raffaello Nemni
IRCCS, Fondazione Don
Carlo Gnocchi, Milan, Italy
Department of
Physiopathology and
Transplants, University of
Milano, Milan, Italy

PD include bradykinesia, muscular rigidity, rest tremor, and postural and gait impairment.¹

The disease is thought to be caused by a complex interplay of both genetic and environmental factors, but the etiology of PD is still largely unknown.² Although still elusive, blood–brain barrier (BBB) disruption has been proposed as a key pathogenic feature of the neurodegenerative mechanisms of the disease.³ Indeed, BBB breakdown affects the integrity of the neurovascular unit (NVU), undermining proper synaptic functioning, information processing and neuronal connectivity.³ BBB dysfunction in PD has been suggested by a number of findings, including extravasated erythrocytes and accumulation of blood-derived proteins in the corpus striatum,⁴ thinning of the capillary endothelial cell layer, and widespread extravascular IgG staining in the subthalamic nucleus.⁵ In addition, neuroimaging studies in PD have shown BBB disruption *in vivo* as indicated both by significantly elevated uptake of [(11)C]-verapamil in the mid-brain,⁶ and the presence of cerebral microbleeds in cortical and subcortical regions.⁷ As the maintenance of the BBB is crucial in neurovascular interactions, a better understanding of the vascular involvement in PD may help to identify new targets for therapies and could lead to the definition of new biomarkers for the diagnosis and/or monitoring of the disease.

In this framework, magnetic resonance imaging (MRI) is a particularly promising technique to investigate the functioning of the NVU. Indeed, arterial spin labeling (ASL) sequences allow for the evaluation of cerebral perfusion in an operator-independent and noninvasive way. In the last decade, studies performed with ASL have shown altered perfusion patterns,⁸ reduced cortical cerebral blood flow (CBF),⁹ and increased arterial transit time in patients with PD.¹⁰ In addition to CBF and arterial transit time, cerebrovascular reactivity (CVR) can be assessed, which reflects the responsiveness of the cerebral vessel to a vasoactive stimulus, regardless of increased metabolic demand. As such, CVR assessment is particularly suitable for the evaluation of the NVU integrity. Despite two recent MRI studies not having shown any CVR alteration in PD patients,^{10,11} previous studies with transcranial Doppler (TCD) reported a reduced vascular reactivity in PD,^{12,13} in agreement with the evidence of BBB alterations that characterize the pathology. To the best of the authors' knowledge, though, this index has never been analyzed in the

specific regions composing the motor circuit, which are primarily involved in the pathogenesis of PD.^{14,15} Given the higher spatial resolution of MRI with respect to the well-established TCD technique, ASL offers the possibility to assess perfusion parameters even in these specific structures.

The aim of this study was to investigate basal perfusion and CVR in PD patients compared with a group of healthy control subjects (HCs), using ASL MRI. The study focused on the cortical and subcortical areas belonging to the motor circuit, analyzing possible correlations between CBF and CVR in these areas, and the severity of motor symptoms quantified with the Unified Parkinson's Disease Rating Scale part III (UPDRS III) score.

Material and methods

Demographic

A total of 28 PD patients and 32 HCs were enrolled for this study. PD patients who participated in the study were consecutively recruited from the Neurorehabilitation Unit of the IRCSS Fondazione Don Gnocchi in Milan. HCs were enrolled either among personnel and volunteers at IRCSS Fondazione Don Gnocchi or among their friends and families. The inclusion criteria were: (1) being either a healthy individual or bearing a diagnosis of probable idiopathic PD according to the Movement Disorder Society Clinical Diagnostic Criteria for PD¹⁶; (2) no psychiatric disorders and/or neurologic disease other than PD; (3) no cardiovascular and/or metabolic diseases. For PD patients, additional inclusion criteria were defined: (1) positive DaTscan; (2) mild to moderate stage of the disease with a scoring between stages 1 and 3 of the Modified Hoehn and Yahr (H&Y) Scale¹⁷; (3) stable drug therapy with either L-Dopa or dopamine agonists; (4) freezing assessed with Unified Parkinson's Disease Rating Scale (UPDRS) part II lower than 2; (5) time spent with dyskinesias assessed with UPDRS part IV lower than 2. Being left-handed was defined as an exclusion criteria.

Demographic information was collected for all the enrolled subjects. For PD participants, the disease stage was quantified with H&Y,¹⁷ and the severity of PD symptoms was assessed with UPDRS, motor part III (UPDRS III) by an experienced neurologist, within 2 weeks of MRI scan. Medications were recorded and levodopa equivalent dose (LEDD) was calculated.¹⁸ Furthermore,

the cognitive performances of all participants with PD were assessed with the Montreal Cognitive Assessment (MoCA) test.

The study was approved by the IRCSS Fondazione Don Carlo Gnocchi Ethics Committee on 1 July 2015 and it was performed in accordance with the principles of the Helsinki Declaration. Written informed consent was obtained from all the subjects before participation in the study.

MRI acquisition

Participants were scanned on a 1.5T Siemens Magnetom Avanto scanner, equipped with a 12-channel head coil.

A dual-echo turbo spin echo proton density PD/T2-weighted scan (repetition time (TR) = 5550 ms, echo time (TE) = 23/103 ms, matrix size = 320 × 320 × 45, resolution 0.8 × 0.8 × 3 mm³) was acquired for all the participants to assess focal white matter (WM) lesions. Furthermore, as anatomical reference, the MRI protocol included: (1) a 3D high-resolution T1-weighted image obtained with a magnetization-prepared rapid acquisition with gradient echo (MPRAGE) sequence (TR = 1900 ms, TE = 3.37 ms, TI = 1100 ms, matrix size = 192 × 256 × 176, resolution 1 × 1 × 1 mm³); (2) a 2D T1-weighted anatomical image with 5 mm thick axial slices (TR/TE = 393/12 ms, matrix size = 128 × 128 × 26, resolution = 1.7 × 1.7 × 5 mm³).

In addition, all the participants were scanned with multi-delay pseudo-continuous ASL (pCASL) sequence with background suppressed 3D gradient and spin echo (GRASE) readout¹⁹ (TR/TE = 3500/22.58 ms, labeling duration = 1500 ms, 5 post-labeling delays (PLD) = [700, 1200, 1700, 2200, 2700] ms, 12 pairs of tag/control images for each delay, matrix size = 64 × 64 × 32, resolution = 3.5 × 3.5 × 5 mm³, distance between the center of imaging slices and labeling plane of 90 mm; 3 M0 images acquired with TR = 5000 ms) to assess basal perfusion.

To assess CVR, for a subgroup of PD and HC participants (13 PD and 13 HCs), multidelay pCASL was acquired twice, first in basal conditions (i.e. at normocapnia), then in hypercapnic normoxic conditions. The hypercapnic stimulus consisted of breathing a gas mixture (5% CO₂, 21% O₂, and 74% N₂) from a Douglas bag through a face mask. The two pCASL scans were acquired without

subject repositioning, by switching the air intake path from the room to the Douglas bag. The acquisition of the second pCASL sequence was performed after 2 minutes from the beginning of the air mixture inhalation to allow reaching steady state. During pCASL scans the end-tidal CO₂ (ETCO₂) was measured with a multigas monitor (Fukuda Denshi Dynascope DS-8100, sampling every 2 seconds) and the heartbeat was monitored with a pulse oximeter.

MRI analysis

All MRI data were visually checked to exclude bad quality scans. Image processing was performed with FMRIB's Software Library (FSL, <http://www.fmrib.ox.ac.uk/fsl>) unless otherwise specified.

WM hyperintensities on PD images were segmented with Jim 6.0 software package (<http://www.xinapse.com/>) by an experienced neuroradiologist. For each subject, the segmented regions of interest (ROIs) were registered to high-resolution 3D T1-weighted image space with Advanced Normalization Tools (ANTs; <http://stnava.github.io/ANTs>), and lesion filling was performed to avoid tissue misclassification during segmentation.²⁰ Gray matter (GM), WM, and cerebrospinal fluid (CSF) were segmented on all 3D T1-weighted image with SIENAX.²¹

All pCASL data (i.e. the one acquired both in normocapnic and in hypercapnic conditions) were processed with the same steps, as follows: (1) tag and control images were realigned, and motion correction was performed with ANTs; (2) CBF maps were estimated with `oxford_asl` tool²² (T1 of blood tissue = 1.2 s, T1 of blood = 1.36 s, tagging efficiency = 0.8)¹⁹; (3) CBF maps were calibrated using `asl_calib` tool,²² adjusting for CSF magnetization extracted from ventricles on M0 images; (4) partial volume effect (PVE) correction was performed (considering GM CBF = 2.5 × WM CBF)²³; (5) GM CBF maps were non-linearly registered to MNI standard space.

For the participants that were scanned with pCASL at both normocapnia and hypercapnia, GM CVR maps were also computed. First, GM PVE-corrected CBF maps derived from ASL data acquired in basal conditions (CBF_{basal}) and in hypercapnic conditions (CBF_{hyperCO₂}) were linearly registered to 2D T1-weighted image with ANTs. In this common space, CVR map was computed as

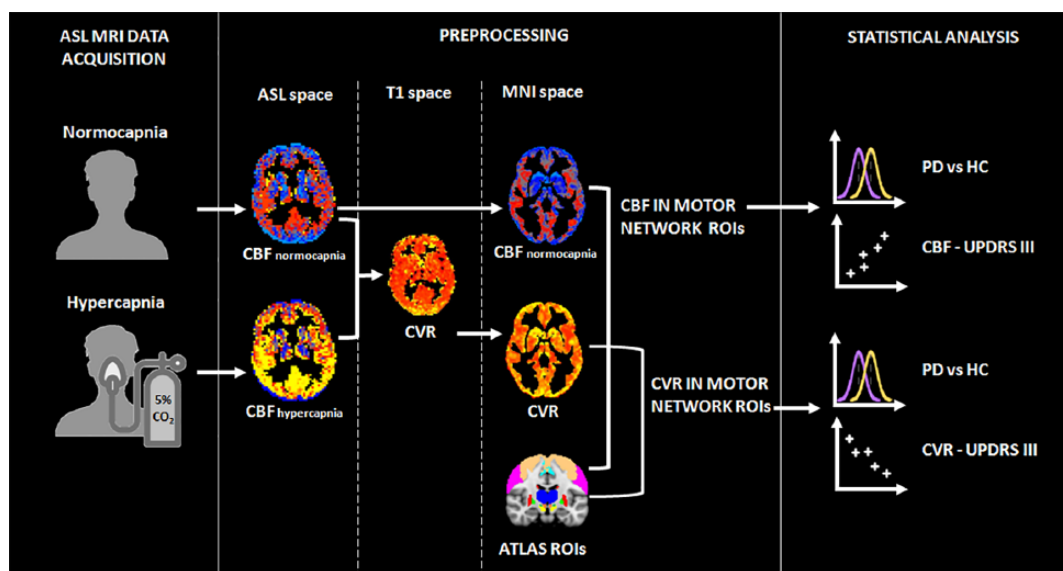


Figure 1. Schematic pipeline of the preprocessing and statistical analysis performed in this study. ASL, arterial spin labelling; CBF, cerebral blood flow; CVR, cerebrovascular reactivity; HC, healthy control; PD, Parkinson's disease; ROI, region of interest; UPDRS III, Unified Parkinson's Disease Rating Scale, part III.

$$\left[\frac{(\text{CBF}_{\text{hyperCO}_2} - \text{CBF}_{\text{basal}})}{\text{CBF}_{\text{basal}}} \right] * 100 / (\text{ETCO}_{2\text{hyperCO}_2} - \text{ETCO}_{2\text{basal}})^{23}$$
, with $\text{ETCO}_{2\text{hyperCO}_2}$ and $\text{ETCO}_{2\text{basal}}$ being the mean ETCO_2 measured for each subject during the acquisition of the two scans. Finally, the obtained CVR maps were non-linearly registered to MNI space using ANTs.

For each enrolled PD patient and HC, median $\text{CBF}_{\text{basal}}$ was extracted within specific cortical and subcortical ROIs of the motor circuit: precentral gyrus, postcentral gyrus, supplementary motor area, striatum, pallidum, thalamus, red nucleus, substantia nigra, and subthalamic nucleus. These ROIs were defined from the Harvard–Oxford atlas,²⁴ except for red nucleus, substantia nigra, and subthalamic nucleus that were derived from the Multi-contrast PD25 atlas.²⁵ For the subgroup of subjects for which CVR maps were computed, median CVR was extracted from the same ROIs. Subcortical ROIs were eroded with a Gaussian kernel ($\sigma = 2\text{mm}$) before performing the $\text{CBF}_{\text{basal}}$ /CVR extraction.

Statistical analysis

Statistical analysis was performed with SPSS (version 24; IBM Corp., Armonk, NY, USA) and Matlab (MATLAB Release 2013a, The MathWorks, Inc., Natick, MA, USA). The normality of data distribution was assessed with Shapiro–Wilk test. Age, sex, and body mass index

(BMI) differences between PD and HC groups, and between PD and HC subgroups, were tested with Student's *t* test and Chi squared test, as appropriate.

For all the ROIs of the motor circuit, $\text{CBF}_{\text{basal}}$ and CVR differences between PD and HC groups were assessed with Mann–Whitney *U* test. The Benjamini–Hochberg procedure was performed to control for the false discovery rate (FDR).

For the PD participants, partial Pearson's correlations between $\text{CBF}_{\text{basal}}$ /CVR and UPDRS III, corrected for age, were computed within all the ROIs of the motor circuit, and corrected for multiple comparisons for the FDR. LEDD was not included as covariate because no significant bivariate correlation was observed between it and $\text{CBF}_{\text{basal}}$ /CVR in the ROIs (results not shown).

FDR-corrected *p* values lower than 0.05 were considered significant. Figure 1 shows a schematic diagram of the pipeline of the whole study.

Results

Participants

Demographic and clinical information of the recruited PD and HC groups are reported in Table 1.

Table 1. Demographics of PD and HC groups. Chi-squared test (a) and independent samples Student's *t* test (b) were used to evaluate differences between PD and HC groups, as appropriate. *p* values lower than 0.05 were considered significant. MoCA scores were corrected according to Conti *et al.*²⁶

	PD (<i>n</i> = 28)	HCs (<i>n</i> = 32)	PD versus HCs <i>p</i> value
Males, <i>n</i> (%)	22 (78.6)	20 (62.5)	0.175 ^a
Age in years, mean (SD)	66.6 (8.6)	63.1 (8.1)	0.111 ^b
BMI, mean (SD)	25.1 (2.1)	24.2 (3.6)	0.306 ^b
H&Y, median (IQR)	1.5 (1–1.9)	–	–
UPDRS III, mean (SD)	19.3 (11.4)	–	–
Disease duration in years, median (IQR)	3 (2–4)	–	–
Onset laterality, left <i>n</i> (%)	11 (39.3)	–	–
Onset symptoms			
tremor, <i>n</i> (%)	12 (42.9)		
bradykinesia, <i>n</i> (%)	7 (25.0)	–	–
motor deficits, <i>n</i> (%)	2 (7.1)		
others, <i>n</i> (%)	7 (25.0)		
LEDD, mean (SD)	214.3 (125.2)	–	–
MoCA, median (IQR)	22.9 (20.0–24.9)	–	–

BMI, body mass index; HC, healthy control; H&Y, Hoehn and Yahr scale; IQR, interquartile range; LEDD, levodopa dose equivalent; MoCA, Montreal Cognitive Assessment; PD, Parkinson's disease; SD, standard deviation; UPDRS III, Unified Parkinson's Disease Rating Scale, part III motor examination total scores.

No significant differences in terms of age (PD mean age \pm standard deviation (SD) = 66.6 \pm 8.6 years, HCs mean age \pm SD = 63.1 \pm 8.1 years), sex (PD: 22 males; HCs: 20 males), and BMI (PD mean BMI \pm SD = 25.1 \pm 2.1, HCs mean BMI \pm SD = 24.2 \pm 3.6) were found between the two groups. The PD group showed a median H&Y (IQR) of 1.5 (1–1.9), a median disease duration (IQR) of 3 (2–4) years and a mean UPDRS III score \pm SD of 19.3 \pm 11.4.

The PD and HC subgroups used in the CVR analysis were also age, sex, and BMI matched (PD mean age \pm SD = 64.5 \pm 9.9 years, HCs mean age \pm SD = 66.3 \pm 9.3; PD: 13 males; HCs: 11 males; PD mean BMI \pm SD = 25.3 \pm 2.4, HCs mean BMI \pm SD = 25.1 \pm 3.4). Demographics for PD and HC subgroups are reported in Supplementary Table 1.

All the acquired images were classified as good quality scans and included in the analysis.

Comparison between PD and HCs

No significant CBF_{basal} differences were observed between PD and HC groups. The median CBF_{basal} and IQR are reported in Supplementary Table 2. Furthermore, no significant CVR difference was observed between PD and HC subgroups. The median CVR and IQR values are reported in Supplementary Table 3.

Partial correlations with UPDRS III

Significant positive partial correlation between CBF_{basal} and UPDRS III, corrected for age, was observed in the PD group within the precentral gyrus (ρ = 0.633, p_{FDR} = 0.001), the postcentral gyrus (ρ = 0.673, p_{FDR} < 0.001), the supplementary motor area (ρ = 0.543, p_{FDR} = 0.003), the corpus striatum (ρ = 0.493, p_{FDR} = 0.015), the pallidum (ρ = 0.447, p_{FDR} = 0.023), the thalamus (ρ = 0.648, p_{FDR} = 0.002), the red nucleus (ρ = 0.555,

Table 2. Partial correlations (corrected for age) between CBF extracted in cortical and subcortical regions of the motor circuit and UPDRS III, in PD patients ($n = 28$). Benjamini–Hochberg procedure was performed to correct for Type I errors. An alpha level of 0.05 was considered significant (in bold).

	rho	p value_{FDR}
Precentral gyrus	0.633	0.001
Postcentral gyrus	0.673	<0.001
Supplementary motor area	0.543	0.003
Striatum	0.493	0.015
Pallidum	0.447	0.023
Thalamus	0.648	0.002
Red nucleus	0.555	0.009
Substantia nigra	0.485	0.015
Subthalamic nucleus	0.135	0.500

CBF, cerebral blood flow; FDR, false discovery rate; PD, Parkinson's disease.

$p_{FDR} = 0.009$), and the substantia nigra ($\rho = 0.485$, $p_{FDR} = 0.015$) (Table 2).

The scatterplots showing the significant correlation between CBF and UPDRS III are represented in Figure 2.

Significant negative partial correlation between CVR and UPDRS III, corrected for age, was observed in the PD subgroup within the striatum ($\rho = -0.720$, $p_{FDR} = 0.048$) (Table 3).

The scatterplot showing the relationship between CVR and UPDRS III in the corpus striatum is reported in Figure 3.

Discussion

In this study CBF and CVR were investigated in a group of patients with tremor-dominant PD,¹ focusing on the motor network. Differences with respect to HCs were tested and the correlation between these perfusion parameters and the severity of PD motor symptoms was assessed. Although no significant difference with HCs was found for CBF and CVR, significant correlations between CBF/CVR and UPDRS III were observed, suggesting neurovascular involvement in PD.

The reported absence of perfusion alterations in PD patients in any considered ROI is a result that has to be interpreted with caution. Previous perfusion assessments in PD were not consistent and reached discordant conclusions. Both hypoperfusion²⁷ and hyperperfusion^{28–30} were reported in the motor cortex by Single Photon Emission Computed Tomography (SPECT) and MRI studies. This inconsistency is mirrored by functional MRI findings, based on the hemodynamics-driven blood oxygen level dependent (BOLD) signal, that showed either hyperactivity,^{31–33} or reduced activation^{34,35} in the motor cortex of PD patients. Owing to neurovascular coupling, neural activation, metabolism, and perfusion are interleaved pathways.¹³ Although reduced cortical perfusion and hypometabolism may be expected in PD as a consequence of dopaminergic neuron damage, an opposite trend of increased CBF and hypermetabolism in the motor cortex could be ascribed either to the motor symptomatology that characterize PD³⁶ or to compensatory mechanisms,³¹ that may be present at the mild to moderate stages of the disease, when complications related to long-term symptomatic treatment are not present.¹ The significant positive correlation that we observed between UPDRS III and CBF in the precentral gyrus, postcentral gyrus, and supplementary motor area in PD patients is in line with the previous findings of hyperperfusion and hyperactivation in cortical regions belonging to the motor circuit, and suggests that mechanisms of functional reorganization could be involved in the early stages of the pathology.³⁷

A significant positive correlation between CBF and UPDRS III was observed also in the basal ganglia, which receive input from, and send output to the cortex through multisynaptic anatomical aggregated loops.^{14,15} This result may be interpreted in the context of previous findings suggesting that the renin–angiotensin system may play an important role in dopamine-mediated neuroinflammation in the nigrostriatal system in PD.³⁸ Increased angiogenesis in the substantia nigra and in subcortical areas was also reported in PD.^{3,39,40} Furthermore, the reduction of dopaminergic neurons has been found to be linked to increased levels of vascular endothelial growth factor (VEGF) and interleukin (IL)-1 β in the striatum,⁴⁰ the crosstalk of which has been previously shown to promote pro-inflammatory and pro-angiogenic cascades.⁴¹ Taken together, these mechanisms leading to vascular reorganization in PD could be related to the

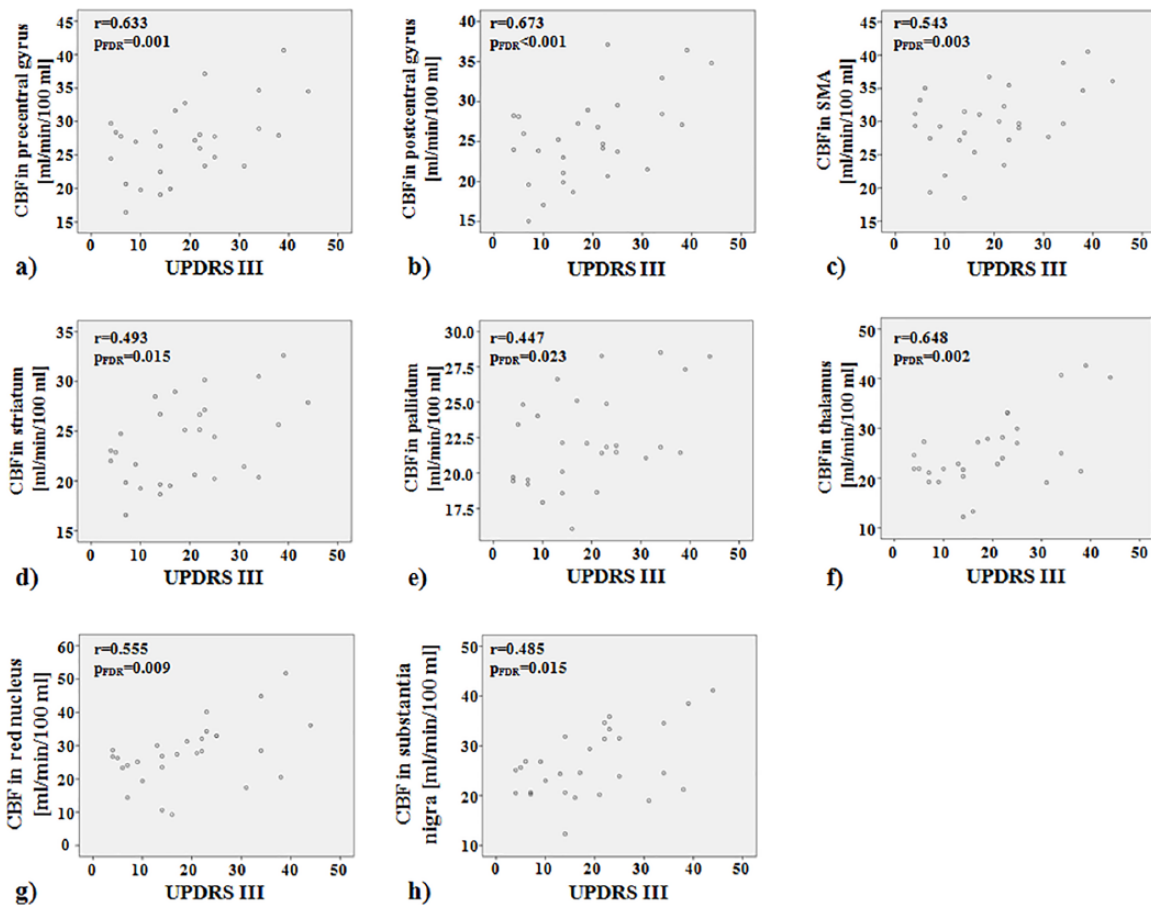


Figure 2. Scatterplots showing significant positive correlations between basal CBF and UPDRS III in PD group ($n = 28$) within the precentral gyrus (a), postcentral gyrus (b), SMA (c), striatum (d), pallidum (e), thalamus (f), red nucleus (g) and substantia nigra (h). CBF, cerebral blood flow; PD, Parkinson's disease; SMA, supplementary motor area; UPDRS III, Unified Parkinson's Disease Rating Scale, part III.

trend for higher CBF in deep GM that we observed in the case of worse PD severity.

In this study, the assessment of NVU integrity was investigated also in terms of CVR, which is a well-established indicator of vascular reserve and autoregulatory efficiency.⁴² In order to perform CVR assessment, a hypercapnic stimulus was administered to a subgroup of the subjects, producing a decrease in vascular resistance and increase in flow without a significant concomitant increase in metabolic rate.⁴² No significant CVR alterations were observed in our PD patients, in line with the only two other studies that investigated CVR with MRI, in cohorts of PD patients with a comparable size to ours (13 subjects the current study, 10 in the study by Krainik *et al.*¹¹ and 14 in Al-Bachari *et al.*¹⁰). Nevertheless, the

significant negative correlation that we found between CVR in the striatum and the severity of motor symptoms hints at CVR alterations in PD. This hypothesis agrees with the findings of two previous studies performed with TCD that reported reduced CVR in PD,^{12,43} and it encourages further investigations.

Interestingly, the significant correlations of UPDRS III and CBF/CVR observed in the striatum have opposite sign, with worse motor symptoms being associated with higher CBF and lower CVR. Evidence from histological studies has shown increased permeability of the BBB,^{4,5} and higher VEGF levels in the corpus striatum in PD.⁴⁰ Therefore, capillaries might be increased in number but more vulnerable in the deep GM in PD.⁴⁴ The significant negative correlation between CVR

Table 3. Partial correlations (corrected for age) between CVR extracted in cortical and subcortical regions of the motor circuit and UPDRS III, in PD patients ($n = 13$). Benjamini–Hochberg procedure was performed to correct for Type I errors. An alpha level of 0.05 was considered significant (in bold).

	rho	p value_{FDR}
Precentral gyrus	-0.589	0.066
Postcentral gyrus	-0.670	0.051
Supplementary motor area	-0.396	0.203
Striatum	-0.720	0.048
Pallidum	-0.310	0.410
Thalamus	-0.575	0.100
Red nucleus	-0.615	0.099
Substantia nigra	-0.448	0.216
Subthalamic nucleus	-0.206	0.521

CVR, cerebrovascular reactivity; FDR, false discovery rate; PD, Parkinson's disease.

and the severity of PD motor symptoms might be further evidence of microvascular changes occurring in the deep GM during the development of the disease. In future studies, assessing CBF/CVR in association with angiogenesis measures, inflammatory marker levels in the blood, and metabolic indexes derived from dopamine transporter imaging could help to clarify the relationship between dopaminergic activity, angiogenesis, and neuroinflammation phenomena in the disease.

The link that was established between CBF/CVR and UPDRS III suggests that these MRI-derived markers might provide additional information for PD diagnosis and monitoring. A better understanding of NVU disruption mechanisms may offer new insight into PD treatment and monitoring.³ For example, in the context of motor rehabilitation that promotes synaptic plasticity in PD,⁴⁵ exercise enhances both the amount of brain-derived neurotrophic factors and vascular health.⁴⁶ Thus, longitudinal assessment of CBF/CVR may provide information about vascular changes due to the treatment. In addition, performing multimodal MRI studies, including also the assessment of other MRI markers (e.g. microstructural integrity parameters derived from diffusion weighted imaging) may

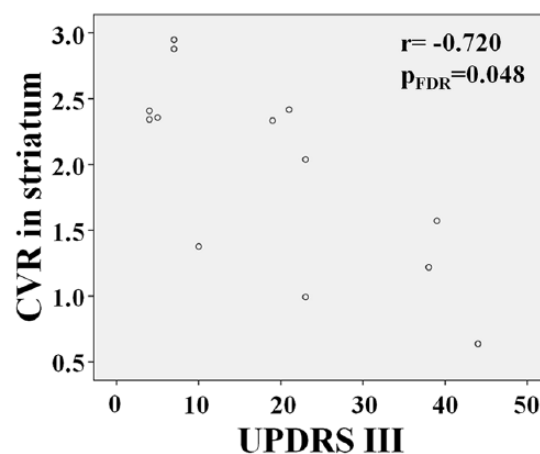


Figure 3. Scatterplot showing significant negative correlation between CVR and UPDRS III in PD subgroup ($n = 13$) within corpus striatum. CVR, cerebrovascular reactivity; PD, Parkinson's disease; UPDRS III, Unified Parkinson's Disease Rating Scale, part III.

allow to identify the relationship between different kind of alterations due to the disease.

The main limitation of this study is the relatively small sample size, which may have prevented us from showing CBF and CVR differences between PD and HC groups. Given the high chance of Type II errors, investigating CBF and CVR in a wider group of subjects is warranted. As there are limited data in the literature regarding perfusion and clinical outcomes in PD, our results can be useful for performing power analyses to guide future studies.

In conclusion, to the best of the authors' knowledge, this is the first study that evaluated CBF and CVR in specific regions of the motor circuit in PD patients. Further investigations will be needed to confirm the results herein, but the observation that CBF and CVR correlate with the severity of motor symptoms in many of the considered ROIs, supports the hypothesis of NVU involvement in PD.

Acknowledgements

We acknowledge the receipt of the software from the University of Southern California's Stevens Neuroimaging and Informatics Institute and The Regents of the University of California, on behalf of its Los Angeles campus.

Funding

This study was funded by a grant awarded by the Annette Funicello Research Fund for Neurological

Diseases and by the Italian Ministry of Health (Ricerca Corrente 2016–2018).

Conflict of interest statement

The authors declare that there is no conflict of interest.

ORCID iDs

Laura Pelizzari  <https://orcid.org/0000-0002-7563-6519>

Francesca Baglio  <https://orcid.org/0000-0002-6145-5274>

Supplemental material

Supplemental material for this article is available online.

References

1. Kalia LV and Lang AE. Parkinson's disease. *Lancet* 2015; 386: 896–912.
2. Alexoudi A, Alexoudi I and Gatzonis S. Parkinson's disease pathogenesis, evolution and alternative pathways: a review. *Rev Neurol* 2018; 174: 699–704.
3. Sweeney MD, Sagare AP and Zlokovic BV. Blood–brain barrier breakdown in Alzheimer disease and other neurodegenerative disorders. *Nat Rev Neurol* 2018; 14: 133–150.
4. Gray MT and Woulfe JM. Striatal blood–brain barrier permeability in Parkinson's disease. *J Cereb Blood Flow Metab* 2015; 35: 747–750.
5. Pienaar IS, Lee CH, Elson JL, *et al.* Deep-brain stimulation associates with improved microvascular integrity in the subthalamic nucleus in Parkinson's disease. *Neurobiol Dis* 2015; 74: 392–405.
6. Kortekaas R, Leenders KL, van Oostrom JC, *et al.* Blood–brain barrier dysfunction in parkinsonian midbrain in vivo. *Ann Neurol* 2005; 57: 176–179.
7. Ham JH, Yi H, Sunwoo MK, *et al.* Cerebral microbleeds in patients with Parkinson's disease. *J Neurol* 2014; 261: 1628–1635.
8. Melzer TR, Watts R, MacAskill MR, *et al.* Arterial spin labelling reveals an abnormal cerebral perfusion pattern in Parkinson's disease. *Brain* 2011; 134: 845–855.
9. Syrimi ZJ, Vojtisek L, Eliasova I, *et al.* Arterial spin labelling detects posterior cortical hypoperfusion in non-demented patients with Parkinson's disease. *J Neural Transm* 2017; 124: 551–557.
10. Al-Bachari S, Parkes LM, Vidyasagar R, *et al.* Arterial spin labelling reveals prolonged arterial arrival time in idiopathic Parkinson's disease. *Neuroimage Clin* 2014; 6: 1–8.
11. Krainik A, Maillet A, Fleury V, *et al.* Levodopa does not change cerebral vasoreactivity in Parkinson's disease. *Mov Disord* 2013; 28: 469–475.
12. Camargo CH, Martins EA, Lange MC, *et al.* Abnormal cerebrovascular reactivity in patients with Parkinson's disease. *Parkinsons Dis* 2015; 2015: 523041.
13. Smolinski L and Czlonkowska A. Cerebral vasomotor reactivity in neurodegenerative diseases. *Neurol Neurochir Pol* 2016; 50: 455–462.
14. Alexander GE and Crutcher MD. Functional architecture of basal ganglia circuits: neural substrates of parallel processing. *Trends Neurosci* 1990; 13: 266–271.
15. Caligiore D, Helmich RC, Hallett M, *et al.* Parkinson's disease as a system-level disorder. *NPJ Parkinsons Dis* 2016; 2: 16025.
16. Postuma RB, Berg D, Stern M, *et al.* MDS clinical diagnostic criteria for Parkinson's disease. *Mov Disord* 2015; 30: 1591–1601.
17. Goetz CG, Poewe W, Rascol O, *et al.* Movement disorder society task force report on the Hoehn and Yahr staging scale: status and recommendations. *Mov Disord* 2004; 19: 1020–1028.
18. Tomlinson CL, Stowe R, Patel S, *et al.* Systematic review of levodopa dose equivalency reporting in Parkinson's disease. *Mov Disord* 2010; 25: 2649–2653.
19. Wang DJ, Alger JR, Qiao JX, *et al.* Multi-delay multi-parametric arterial spin-labeled perfusion MRI in acute ischemic stroke - Comparison with dynamic susceptibility contrast enhanced perfusion imaging. *Neuroimage Clin* 2013; 3: 1–7.
20. Gelineau-Morel R, Tomassini V, Jenkinson M, *et al.* The effect of hypointense white matter lesions on automated gray matter segmentation in multiple sclerosis. *Hum Brain Mapp* 2012; 33: 2802–2814.
21. Smith SM, Zhang Y, Jenkinson M, *et al.* Accurate, robust, and automated longitudinal and cross-sectional brain change analysis. *Neuroimage* 2002; 17: 479–489.
22. Chappell MA, Groves AR, Whitcher B, *et al.* Variational Bayesian inference for a nonlinear forward model. *IEEE Trans Signal Proc* 2009; 57: 223–236.

23. Marshall O, Lu H, Brisset JC, *et al.* Impaired cerebrovascular reactivity in multiple sclerosis. *JAMA Neurol* 2014; 71: 1275–1281.
24. Frazier JA, Chiu S, Breeze JL, *et al.* Structural brain magnetic resonance imaging of limbic and thalamic volumes in pediatric bipolar disorder. *Am J Psychiatry* 2005; 162: 1256–1265.
25. Xiao Y, Fonov V, Beriault S, *et al.* Multi-contrast unbiased MRI atlas of a Parkinson's disease population. *Int J Comput Assist Radiol Surg* 2015; 10: 329–341.
26. Conti S, Bonazzi S, Laiacina M, *et al.* Montreal Cognitive Assessment (MoCA)-Italian version: regression based norms and equivalent scores. *Neurol Sci* 2015; 36: 209–214.
27. Kikuchi A, Takeda A, Kimpara T, *et al.* Hypoperfusion in the supplementary motor area, dorsolateral prefrontal cortex and insular cortex in Parkinson's disease. *J Neurol Sci* 2001; 193: 29–36.
28. Matsui H, Udaka F, Miyoshi T, *et al.* Brain perfusion differences between Parkinson's disease and multiple system atrophy with predominant parkinsonian features. *Parkinsonism Relat Disord* 2005; 11: 227–232.
29. Madhyastha TM, Askren MK, Boord P, *et al.* Cerebral perfusion and cortical thickness indicate cortical involvement in mild Parkinson's disease. *Mov Disord* 2015; 30: 1893–1900.
30. Barzgari A, Sojkova J, Maritza Dowling N, *et al.* Brain Imaging and Behavior (2018). <https://doi.org/10.1007/s11682-018-9877-1> First Online 09 May 2018.
31. Mallol R, Barros-Loscertales A, Lopez M, *et al.* Compensatory cortical mechanisms in Parkinson's disease evidenced with fMRI during the performance of pre-learned sequential movements. *Brain Res* 2007; 1147: 265–271.
32. Caproni S, Muti M, Principi M, *et al.* Complexity of motor sequences and cortical reorganization in Parkinson's disease: a functional MRI study. *PLoS One* 2013; 8: e66834.
33. Hughes LE, Barker RA, Owen AM, *et al.* Parkinson's disease and healthy aging: independent and interacting effects on action selection. *Hum Brain Mapp* 2010; 31: 1886–1899.
34. Tessa C, Lucetti C, Diciotti S, *et al.* Hypoactivation of the primary sensorimotor cortex in de novo Parkinson's disease: a motor fMRI study under controlled conditions. *Neuroradiology* 2012; 54: 261–268.
35. Baglio F, Blasi V, Falini A, *et al.* Functional brain changes in early Parkinson's disease during motor response and motor inhibition. *Neurobiol Aging* 2011; 32: 115–124.
36. Yu H, Sternad D, Corcos DM, *et al.* Role of hyperactive cerebellum and motor cortex in Parkinson's disease. *Neuroimage* 2007; 35: 222–233.
37. Tuovinen N, Seppi K, de Pasquale F, *et al.* The reorganization of functional architecture in the early-stages of Parkinson's disease. *Parkinsonism Relat Disord* 2018; 50: 61–68.
38. Labandeira-Garcia JL, Rodriguez-Pallares J, Dominguez-Meijide A, *et al.* Dopamine–angiotensin interactions in the basal ganglia and their relevance for Parkinson's disease. *Mov Disord* 2013; 28: 1337–1342.
39. Barcia C, Bautista V, Sanchez-Bahillo A, *et al.* Changes in vascularization in substantia nigra pars compacta of monkeys rendered parkinsonian. *J Neural Transm* 2005; 112: 1237–1248.
40. Munoz A, Garrido-Gil P, Dominguez-Meijide A, *et al.* Angiotensin type 1 receptor blockage reduces l-dopa-induced dyskinesia in the 6-OHDA model of Parkinson's disease. Involvement of vascular endothelial growth factor and interleukin-1beta. *Exp Neurol* 2014; 261: 720–732.
41. Voronov E, Carmi Y and Apte RN. The role IL-1 in tumor-mediated angiogenesis. *Front Physiol* 2014; 5: 114.
42. Juttukonda MR and Donahue MJ. Neuroimaging of vascular reserve in patients with cerebrovascular diseases. *Neuroimage* 2019; 187 :192–208.
43. Hamdy MM, Sadallah HM and Elsalamawy DH. The study of vasoreactivity of the cerebral vessels in patients with Parkinson disease. *Egypt J Neurol Psychiatry Neurosurg* 2012; 49.
44. Elgayar SAM, Abdel-Hafez AAM, Gomaa AMS, *et al.* Vulnerability of glia and vessels of rat substantia nigra in rotenone Parkinson model. *Ultrastruct Pathol* 2018; 42: 181–192.
45. Petzinger GM, Fisher BE, McEwen S, *et al.* Exercise-enhanced neuroplasticity targeting motor and cognitive circuitry in Parkinson's disease. *Lancet Neurol* 2013; 12: 716–726.
46. Spires-Jones TL and Ritchie CW. A brain boost to fight Alzheimer's disease. *Science* 2018; 361: 975–976.